Journal of Fluorescence (2019) 29:737–749
https://doi.org/10.1007/s10895-019-02382-4

ORIGINAL ARTICLE

Turn-on Fluorescence Chemosensor for Zn^{2+} Ion Using Salicylate Based Azo Derivatives and their Application in Cell-Bioimaging

Mathappan Mariyappan[1] · Nelson Malini[1] · Jayaraman Sivamani[1] · Gandhi Sivaraman[1] · Muniyasamy Harikrishnan[1] · Sepperumal Murugesan[1] · Ayyanar Siva[1]

Received: 29 January 2019 / Accepted: 17 April 2019 / Published online: 23 May 2019

Abstract

The synthesis and optical studies of salicylate based azo derivatives (DPSAD and IPSAD) are reported. The receptors act as a versatile fluorogenic chemosensor for Zn^{2+} causing a selective enhancement of fluorescence over other competing cations. The complex formed between receptors and Zn^{2+} are identified on the basis of absorption and fluorescence titration and further confirmed by ESI-MS. DFT/TD-DFT calculations support the observed optical changes happens only upon complexation with Zn^{2+} ion. Moreover, receptors are further applied to intracellular sensing and imaging studies.

Keywords Azo derivatives · Salicylate derivative · Chemosensor · Intracellular sensing · Zinc ion

Introduction

The aim and synthesis of chemosensor exhibit excellent selective and sensitive detection of heavy metal ions in the field of supramolecular, medicinal and environmental chemistry [1–4]. Recently, detailed consciousness has been focused on objective of important selective sensor of metal ions and their recognition of living cell environment [5–9] The findings of trace metal ions have garnered great attention in the past two decades, due to large potential applications in the areas of life sciences, medicinal and biotechnology [10–12]. It is well identified that metal ions play an vital role in biological enzymatic systems. Among the metal ions, specifically zinc (Zn^{2+}) is the second most abundant metal ion (concentration ranging from sub-nM to 0.3 mM) [13] and makes variety of roles in biological system, such as gene expression, apoptosis, metalloenzymes regulation and neurotransmission, [14, 15] neurological diseases, including Alzheimer's, ischemia and epilepsy [16–18] are associated with the disorder of the Zn^{2+} metabolism and also involved in carboxy peptidase and carbonic anhydrase enzymes, which are very important to the regulation of carbon dioxide (CO_2) and digestion of proteins, respectively. In addition, the elevated levels of Zn^{2+} ions in water lead to environmental pollution, viz., decrease the soil microbial activity causing phytotoxic effects, making the water smelly and muddy [19, 20]. Therefore, the design and development of efficient fluorescent chemosensors for selective detection of Zn^{2+} ions are more considerable interest recently. Many Zn^{2+} chemosensors have been reported so far by researchers using fluorophores such as quinoline and its derivatives [21–24], coumarin [25], triazole [26], cyanine [27, 28], rhodamine [29], fluorescein [30, 31], benzophenoxazone [32], anthracene [33, 34], naphthalimide [35–37], BODIPY [38, 39], NBD derivatives [40–43], thiazole derivatives [44] and other near-infrared fluorophores and so on [45]. However, all these probes contain imine

Electronic supplementary material The online version of this article (https://doi.org/10.1007/s10895-019-02382-4) contains supplementary material, which is available to authorized users.

✉ Ayyanar Siva
drasiva@gmail.com; siva.chem@mkuniversity.org

[1] Supramolecular and Organometallic Chemistry Lab, Department of Inorganic Chemistry, School of Chemistry, Madurai Kamaraj University, Madurai, Tamil Nadu 625 021, India

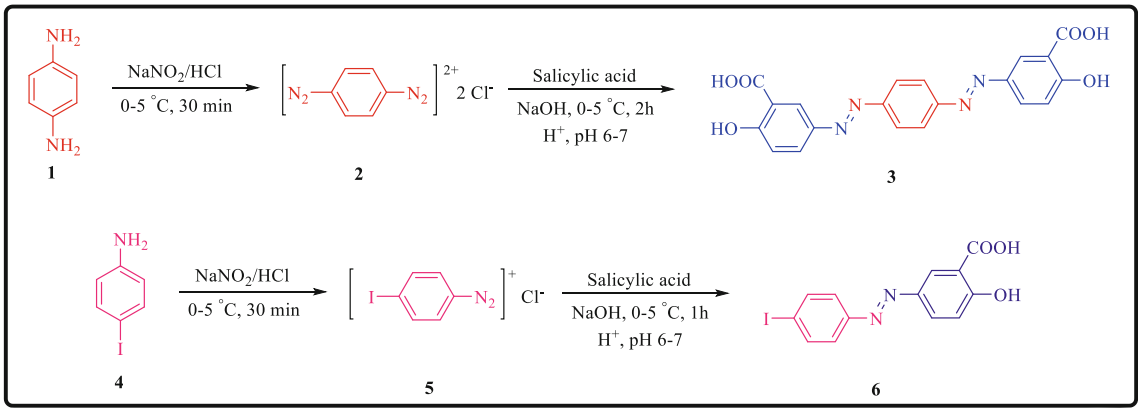

Scheme 1 Synthetic route of salicylate based azo derivatives 3 (DPSAD) and 6 (IPSAD)

N- and carbonyl O-donor atoms are used to binding the metal ions very precisely [46]. Nevertheless, most of the Zn^{2+} chemosensors reported have some disadvantages also such as multi-ion detection [47, 48], a requirement of organic solvent for sensing [49, 50] and interferences from other similar metal ion having similar properties [51–54]. Furthermore, some of the receptors often require relatively tedious synthetic procedure followed by their complex formation and purification [5, 55]. Recently, many improvement has been made in the progress of salicylhydrazide derivative systems with great diversity in this field. Zhefeng et al., and Shouzhi Pu et al., was reported salicylhydrazide based chemosensor for selective sensing for Cu^{2+} and Zn^{2+} ions [56, 57]. Furthermore, Murugavel et al., reported dual sensing ability for picric acid and CO_2 capture by using azo-linked fluorescent triphenylbenzene based covalent organic polymers [58]. As a consequence, much efforts has been dedicated to the development of salicylate based azo chemosensors for the recognition of Zn^{2+} ions [26–29].

In this work, simple salicylate based azo derivatives such as **3** (DPSAD) and **6** (IPSAD) were synthesized and they acts as fluorescent chemosensor for selective detection of Zn^{2+} in aqueous media and living HeLa cells. Further, their photophysical properties and sensing abilities of the receptors have been explored systematically through UV-vis absorption and emission spectra. Both receptors DPSAD and IPSAD demonstrated high selectivity towards Zn^{2+} via the turn-on fluorescence mechanism in the presence of other transition and non-transition metal ions in aqueous media. To the best of our knowledge, no report on salicylate based azo derivatives "turn-on" fluorogenic probe for selective and effective detection of Zn^{2+} ions.

Experimental Section

Materials and Methods

All the chemicals and reagents were used in the present work as an analytical grade. 4-Iodoaniline and 1,4-diaminobenzene were acquired from Alfa Aesar. $NaNO_2$,

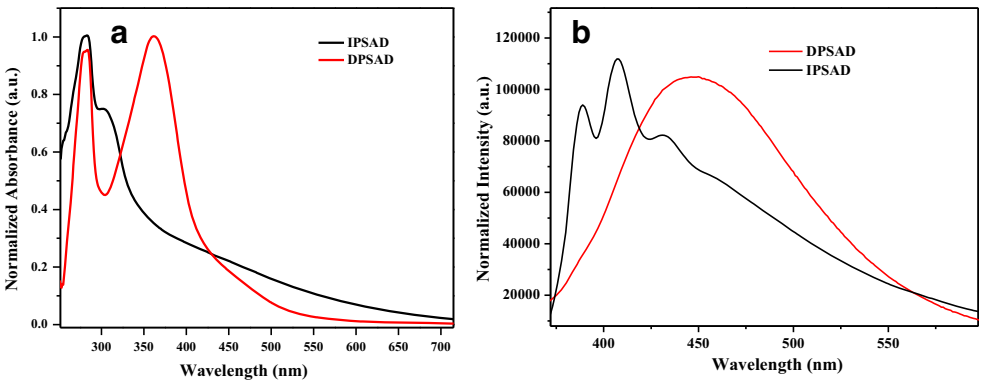

Fig. 1 Normalized absorption (**a**) and emission (**b**) spectra of DPSAD (3) and IPSAD (6) in THF (10 μM)

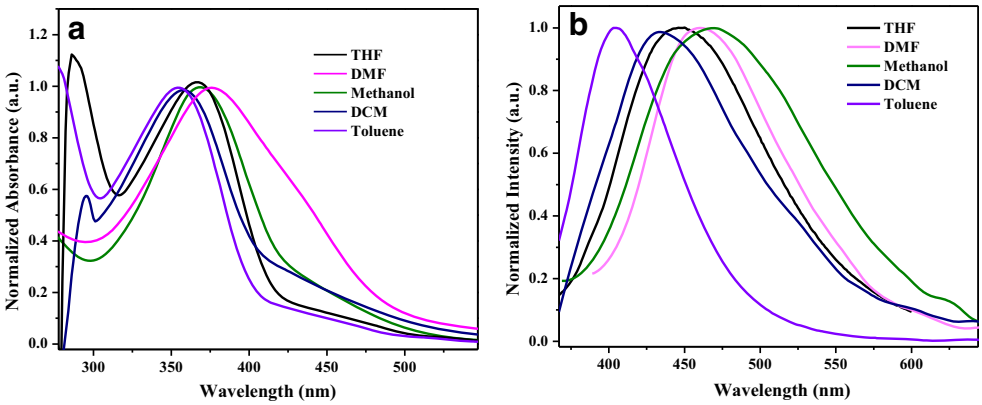

Fig. 2 Normalized absorption (**a**) and emission (**b**) spectra of DPSAD in different organic solvents

HCl, NaOH and metal chloride salts were purchased from Merck and all the common solvents were received from laboratory and analytical grade.

The melting points were calculated in open capillary tubes and are uncorrected. The ^{1}H and ^{13}C NMR spectra were recorded on a Bruker (Avance) 300 MHz NMR instrument using TMS as an internal reference, DMSO-d_6 as a solvent. Standard Bruker software was used throughout. Chemical shift value are given in parts per million (δ-scale) and their coupling constants are specified in Hertz. Silica gel-G plates (Merck) were used for TLC analysis with a mixture of n-hexane and ethyl acetate as mobile phase. Electrospray Ionization Mass Spectrometry (ESI-MS) analyses were recorded in LCQ Fleet, Thermo Fisher Instruments Limited, United States. ESI-MS was measured in positive ion mode. The collision voltage and ionization voltage were − 70 V and − 4.5 kV, respectively, using nitrogen as atomization and desolvation gas. The desolvation temperature was set at 300 °C. The relative amount of each part was determined from the LC-MS chromatogram, using the area normalization method. UV-vis absorption spectra were analysed on JASCO V-630 in 1 cm path length quartz cuvette with a volume of 2 mL at ambient temperature. All fluorescence studies were recorded on a Fluoromax-4 Spectrofluorometer (HORIBA JOBIN YVON) with excitation slit set at 5.0 nm band pass and emission at 5.0 nm band pass in 1 cm × 1 cm quartz cell. The ground-state geometries were optimized using density functional theory with B3LYP hybrid functional at the basis set level of 6-31G. All the calculations were performed using Gaussian 09 package.

Synthesis and Characterization

General Procedure a for Synthesis of Compounds 3 (DPSAD) and 6 (IPSAD)

Aromatic amine was taken in 1:1 ratio of concentrated hydrochloric acid and water. Sodium nitrite solution was added drop wisely into the reaction mixture with constant stirring. The mixture was stirred for about 30 min at a temperature of 0 to 5 °C. The diazotization step was pursued by coupling of the diazotized amines with drop

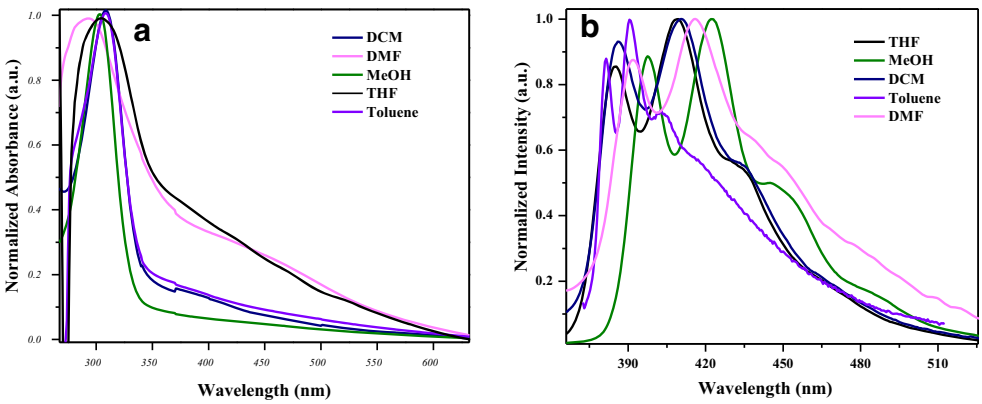

Fig. 3 Normalized absorption (**a**) and emission (**b**) spectra of IPSAD in different organic solvents

Table 1 The photophysical values of DPSAD (3) and IPSAD (6) in different organic solvents

Solvents	DPSAD			IPSAD		
	λ_{abs} (nm)	λ_{emi} (nm)	Stoke's shift (cm^{-1})	λ_{abs} (nm)	λ_{emi} (nm)	Stoke's shift (cm^{-1})
Toluene	354	404	3496	308	391	6897
THF	364	448	5151	304	406	8264
DCM	358	434	4888	306	410	8289
DMF	372	462	5236	295	416	9416
Methanol	369	470	5823	302	422	9898

wise addition to the solution of sodium salicylate. The reaction was stirred at 0–5 °C for about 2 h under basic medium. The resultant azo derivatives (**3** and **6**) were obtained as an orange to red powders after changing the pH range between 6 and 7.

Synthesis of Compound 3 (DPSAD)

Compound **3** (DPSAD) was synthesized by using the above said general procedure **A** using 1,4-diaminobenzene **1** (1 g, 0.092 mmol), $NaNO_2$ (1.28 g, 0.184 mmol), salicylic acid (2.55 g, 0.184 mmol), NaOH (1.48 g, 0.37 mmol). Orange to red solid was obtained (69% yield); m.p 265 °C. FT-IR (cm^{-1}) 3227, 3026, 2834, 2525, 1656, 1606, 1480, 1440, 1382, 1324, 1241, 1205; ^{1}H NMR (300 MHz, DMSO-d_6) $\delta_H = 8.28$ (s, 1H), 7.89 (s, 4H), 7.81 (d, $J = 7.8$ Hz, 2H), 6.79 (d, $J = 6.79$ Hz, 2H); ^{13}C NMR (75 MHz, DMSO-d_6) δ_C 172.73, 162.04, 152.50, 145.94, 128.21, 124.13, 122.67, 119.83, 117.80; ESI-MS: m/z calculated for $C_{20}H_{14}N_4O_6$ 406.0913; found 407.0091 $[M + H]^+$.

Synthesis of Compound 6 (IPSAD)

Compound **6** (IPSAD) was synthesized by using the above said general procedure **A** using 4-iodoaniline **4** (1 g, 0.045 mmol), $NaNO_2$ (0.31 g, 0.045 mmol), salicylic acid (0.63 g, 0.045 mmol), NaOH (0.36 g, 0.091 mmol). Orange to red solid was obtained (65% yield); m.p 232 °C. FT-IR (cm^{-1}) 3216, 2241, 2180, 1571, 1456, 1385, 1339, 1297, 1250, 1172; ^{1}H NMR (300 MHz, DMSO-d_6) $\delta_H = 8.28$ (s, 1H), 7.90 (d, $J = 7.9$ Hz, 2H), 7.81 (d, $J = 7.8$ Hz, 1H), 7.59 (d, $J = 7.58$ Hz, 2H), 6.80 (d, $J = 6.79$ Hz, 1H); ^{13}C NMR (75 MHz, DMSO-d_6) δ_C 172.73, 168.05, 152.50, 143.98, 140.19, 139.01, 127.42, 124.75, 120.06, 118.55, 97.39; ESI-MS: m/z calculated for $C_{13}H_9IN_2O_3$ 367.9658; found 368.9732 $[M + H]^+$.

Results and Discussion

Synthesis of Fluorophores

The synthetic way of two different salicylate based azo compounds **3** (DPSAD) and **6** (IPSAD) are represented in Scheme 1. The anilines **1** and **4** were first diazotized using sodium nitrite in the presence of hydrochloric acid and further it reacts with salicylic acid to afford compounds **3** and **6** with 69% and 65% yields respectively. Both the final compounds were thoroughly characterized by various spectral techniques such as ^{1}H, ^{13}C NMR, FT-IR and ESI-mass spectra.

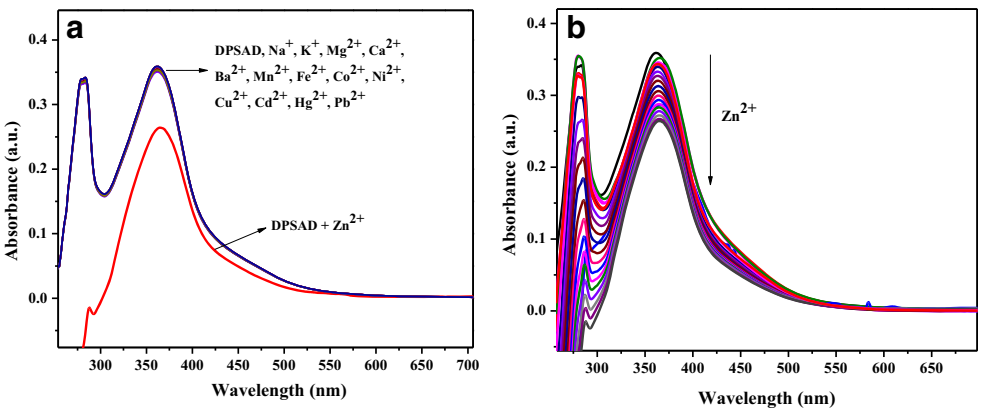

Fig. 4 UV-vis spectra of DPSAD (10 μM) (**a**) with various cations (1×10^{-4} M); (**b**) upon gradual addition of Zn^{2+} (0–20 μM) in aqueous THF (THF/H_2O = 8:2) at pH = 7.4 [HEPES buffer (20 mM)]

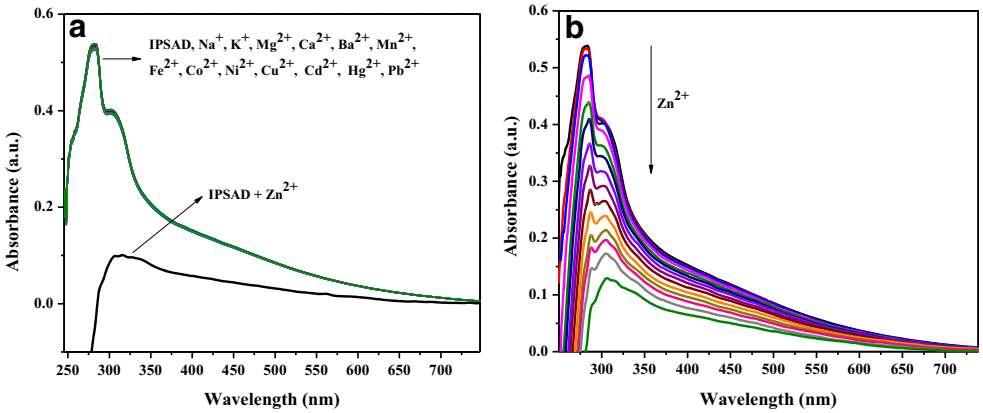

Fig. 5 UV-Vis spectra of IPSAD (10 μM) (**a**) with various cations (1×10^{-4} M); (**b**) upon gradual addition of Zn^{2+} (0–10 μM) in aqueous THF (THF/H_2O = 8:2) at pH = 7.4 [HEPES buffer (20 mM)]

Photophysical Properties

The absorption and emission spectra of **3** (DPSAD) and **6** (IPSAD) in THF are somewhat different to each other (Fig. 1) due to the existence of diazo group in DPSAD (Scheme 1). Both the compounds exhibit two absorption maxima, **3** (DPSAD) appeared at 283 nm and 363 nm while **6** (IPSAD) displayed band at 286 nm and 304 nm. DPSAD shows bathochromic shift from IPSAD this might be due to azo existence. In the emission spectra, compound **3** (DPSAD) showed λ_{emi} at 448 nm (λ_{exi} = 363 nm) and compound **6** (IPSAD) revealed λ_{emi} at 388, 406 and 433 nm (λ_{exi} = 304 nm).

As shown in Figs. 2a and 3a, the nature of solvent polarity is strongly influenced the optical properties of **3** (DPSAD) and **6** (IPSAD), this may be due to the presence of the donor and acceptor groups present in the receptors. The absorption bands of **3** and **6**, are almost negligible shift was noticed, because the ground-state electronic structure and tiny dipole moments coupled with the ICT transitions are self-governing of solvent polarity. As shown in Figs. 2b and 3b, DPSAD and IPSAD depends on the nature of solvent polarity in the emission spectra, this may be due to the presence of the donor and acceptor groups present in the probe. The absorption bands of **3** and **6** has negligible shift because the ground-state electronic structure and tiny dipole moments coupled with the ICT transitions are self-governing of solvent polarity [59]. But in the case of the emission, band was slightly red shifted upon varying the solvent polarity from nonpolar to polar (Figs. 2b and Fig. 3b). This may be due to increase in charge separation at the excited state. In addition to that the absorption spectra of Figs. 2a and Fig. 3a showed a distinct shoulder, thia may be due to the solvent relaxation. We did not find any shoulder peak in the emission spectra. After excitation, the internal charge transfer occurred and causes a highly polar charge separated emission state which is stabilized most effectively by the polar solvents [59] and bathochromic shift also observed. Further, we calculated Stoke's shift values of all the solvents and are listed in (Table 1), we observed that the values are gradually increases from non-polar to polar solvents which indicates that stabilization occurs at highly polar emitting exited state, i.e. the electronic redistribution occurred upon excitation [60].

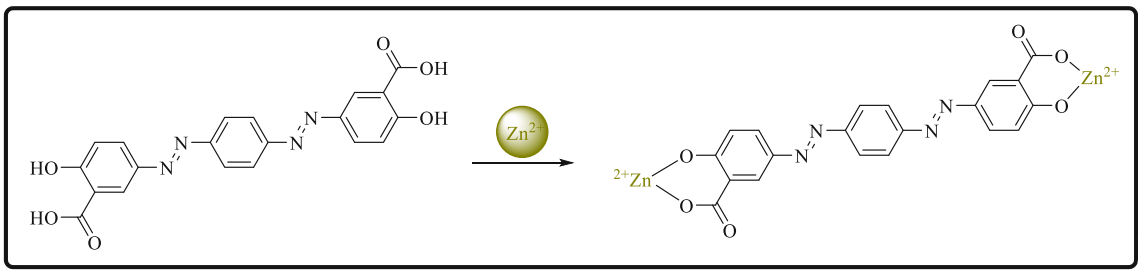

Scheme 2 Probable binding mode of DPSAD with Zn^{2+}

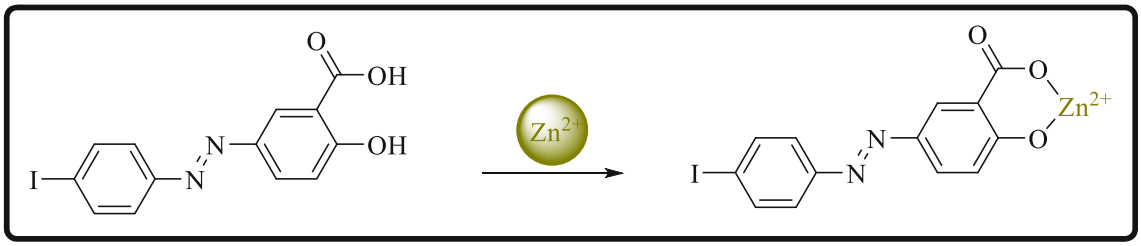

Scheme 3 Probable binding site of IPSAD with Zn^{2+}

Selectivity of DPSAD (3) and IPSAD (6) for Zn^{2+} over Other Competitive Ions

The availability of -COOH and –OH unit of **3** and **6** can act as binding sites towards various metal ions such as K^+, Mg^{2+}, Ca^{2+}, Ba^{2+}, Mn^{2+}, Fe^{2+}, Co^{2+}, Ni^{2+}, Cu^{2+}, Cd^{2+}, Hg^{2+}, Pb^{2+} and Zn^{2+}. The metal binding properties of DPSAD and IPSAD were examined by absorption and emission spectra, in aqueous THF (THF/H_2O = 8:2) at pH = 7.4 [HEPES buffer (20 mM)] at ambient temperature. Initially, the absorption spectrum of DPSAD exhibited two bands at 283 and 363 nm whereas IPSAD displayed bands at 283 and 304 nm in THF/H_2O = 8:2) at pH = 7.4 [HEPES buffer (20 mM)] at ambient temperature. Then, we added the 20 μM and 10 μM of metal ion concentrations into the solution of DPSAD and IPSAD respectively. Under these circumstances metal ions such as Na^+, K^+, Mg^{2+}, Ca^{2+}, Ba^{2+}, Mn^{2+}, Fe^{2+}, Co^{2+}, Ni^{2+}, Cu^{2+}, Cd^{2+}, Hg^{2+} and Pb^{2+} unsuccessful to perform like Zn^{2+}, indicating that both the compounds (DPSAD and IPSAD) acts as competent and discriminating sensor for Zn^{2+} over other essential metal ions (Figs. 4a and Fig. 5a). To determine the coordination behaviour of DPSAD and IPSAD with Zn^{2+}, the UV-vis titration test was carried out alone and given in Figs. 4b and Fig. 5b. From this spectra, when increasing the addition of Zn^{2+} ions to the solution of receptors caused a simultaneous decrease in both the absorption bands which indicates that the formation of co-ordination between receptors and metal ion (Schemes 2 and 3).

The fluorescence titration of the receptors DPSAD and IPSAD in the presence of various metal cations viz., Na^+, K^+, Mg^{2+}, Ca^{2+}, Ba^{2+}, Mn^{2+}, Fe^{2+}, Co^{2+}, Ni^{2+}, Cu^{2+}, Cd^{2+}, Hg^{2+}, Pb^{2+} as well as Zn^{2+} were studied in aqueous THF (THF/H_2O = 8:2) at pH = 7.4 [HEPES buffer (20 mM)]. When the incremental addition of addition of 20 μM and 10 μM of metal ion concentrations to the solution of DPSAD and IPSAD, the fluorescence enhancement gradually increases with blue shift upon excitation at 363 nm (Figs. 6a and Fig. 7). Similarly, when the IPSAD is titrated with Zn^{2+}, fluorescence enhancement is observed with excitation at 304 nm (Fig. 8a). Further, the test solution shows an apparent fluorescence change from red to blue for DPSAD (Fig. 8b) while light yellow to light blue for IPSAD (Fig. 6b) under the irradiation of UV light at 365 nm. To the selectivity test, the addition of other metal ions such as Na^+, K^+, Mg^{2+}, Ca^{2+}, Ni^{2+}, Mn^{2+}, Cu^{2+}, Cd^{2+}, Hg^{2+}, Ba^{2+}, Fe^{2+}, Co^{2+} and Pb^{2+} over the receptors DPSAD and IPSAD were checked and it does not show any observable fluorescence changes (Figs. 6a and Fig. 7a). However, the addition of Zn^{2+} (0–20 μM)

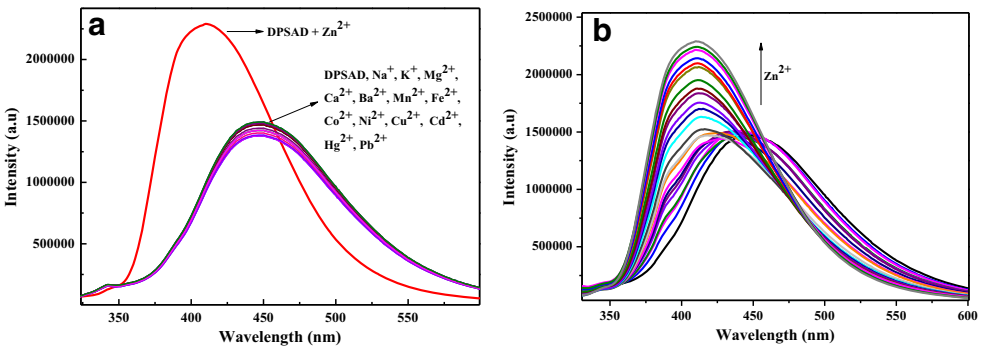

Fig. 6 Emission spectra of DPSAD (10 μM) (**a**) with various cations (1×10^{-4} M); (**b**) upon gradual addition of Zn^{2+} (0–20 μM) in aqueous THF (THF/H_2O = 8:2) at pH = 7.4 [HEPES buffer (20 mM)]. Excitation at 363 nm. Slit width is 5 nm

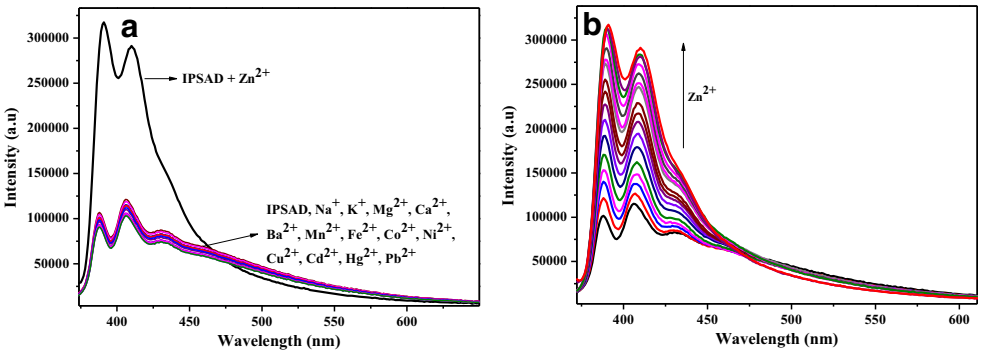

Fig. 7 Emission spectra of IPSAD (10 μM) (**a**) with various cations (1×10^{-4} M); (**b**) upon gradual addition of Zn^{2+} (0–10 μM) in aqueous THF (THF/H_2O = 8:2) at pH = 7.4 [HEPES buffer (20 mM)]. Excitation at 304 nm. Slit width is 5 nm

induced intense fluorescence augmentation with blue shift from 448 nm to 410 nm for DPSAD (Fig. 6b). In case of receptor IPSAD, after titration with Zn^{2+} (0–10 μM), the intensity of emission band at 388, 406 and 433 nm significantly increases without any change in emission wavelength (Fig. 7b), which indicates that the fluorescence intensity changes might be attributed to combine the effect of chelation enhanced fluorescence (CHEF) and intramolecular charge transfer (ICT) within the receptor [25]. From the observed results of the absorption and fluorescence, it is identified that the receptors (DPSAD and IPSAD) are very selective and sensitive for Zn^{2+} over other mono/divalent metal ions such as Na^+, K^+, Ni^{2+}, Cu^{2+}, Ba^{2+}, Mn^{2+}, Cd^{2+}, Hg^{2+}, Mg^{2+}, Ca^{2+}, Fe^{2+}, Co^{2+} and Pb^{2+}.

To test the practical applicability of our newly synthesized receptors (DPSAD and IPSAD), a competitive binding test was studied in the presence of varying concentration of Zn^{2+} with competing analytes. No significant difference was detected in the presence of other competitive ions over the comparison to a solution containing Zn^{2+} metal ion (Fig. 9). These findings suggest that Zn^{2+} recognition by receptors are hardly affected by other synchronized metal ions.

Further, we calculated linear dependent coefficient (R^2) of DPSAD and IPSAD with Zn^{2+} are 0.9976 and 0.9986 respectively with the help of varying concentration of Zn^{2+} ion (Fig. S8). The detection limits of DPSAD and IPSAD were measured to be 6.73×10^{-6} M and 5.07×10^{-6} M for Zn^{2+} which was quite appreciable when compared to those previously reported receptor [61] for Zn^{2+}. The stoichiometry test of

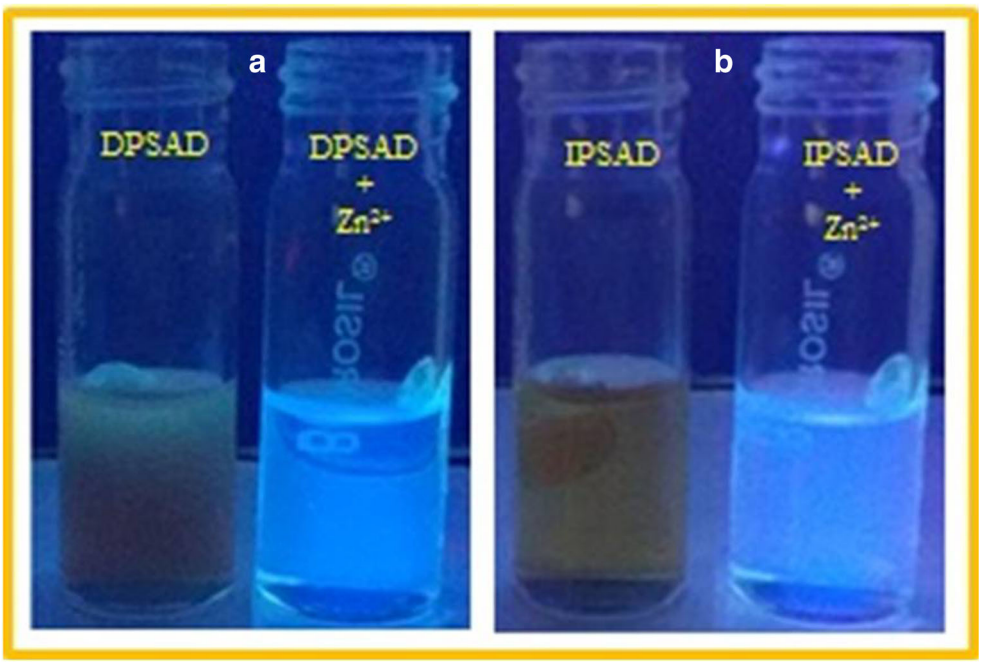

Fig. 8 Fluorescence image of DPSAD and IPSAD with Zn^{2+} under illumination of UV light at 365 nm

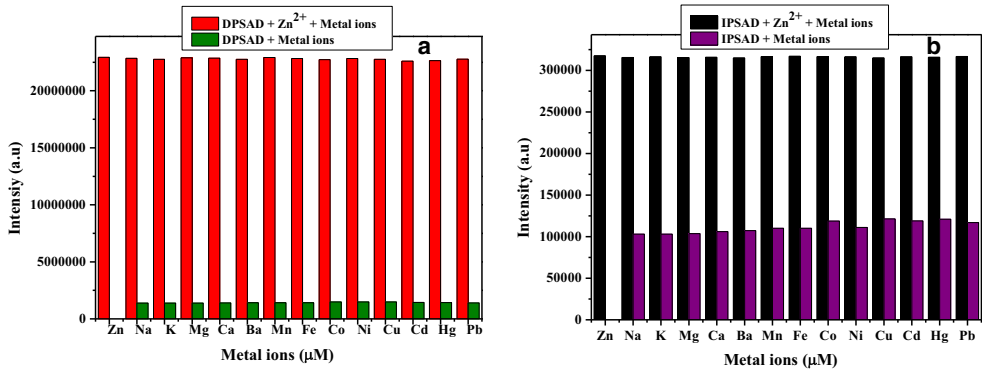

Fig. 9 **a** Selectivity studies of DPSAD and IPSAD with Zn^{2+} (**b**) competitive experiments of DPSAD and IPSAD with Zn^{2+}. Excitation was performed at 363 and 404 nm for DPSAD and IPSAD respectively

DPSAD and IPSAD was carried out with Zn^{2+} and it was estimated by Job's plot using fluorometric titrations with varying concentration of metal ion. From the Job's plot analysis, we observed that DPSAD forms a 1:2 stoichiometric complex and IPSAD forms 1:1 stoichiometric complex with Zn^{2+} (Fig. S9). In order to validate the stoichiometric complex, the efficient bindings of (DPSAD and IPSAD) with Zn^{2+} were studied by ESI-MS. The ESI-MS spectra, (Fig. S10 and Fig. S11) shows peaks at m/z = 530.9247 and 430.8865 corresponding to $[DPSAD+H+2\ Zn^{2+}]^+$ and $[IPSAD+H+Zn^{2+}]^+$ respectively, which also confirmed the formation of 1:2 complex for DPSAD and 1:1 complex for IPSAD with Zn^{2+}.

In biological applications, a suitable pH condition was identified for our newly synthesized the receptors DPSAD and IPSAD and it was evaluated by recording the fluorescence spectra over different pH values (Fig. 10). In acidic condition, (pH 1–4) the fluorescence intensity decreased due to the protonation of receptor but under basic conditions (pH 10–14), the fluorescence intensity of probe enhanced due to the deprotonation of salicylate (-COOH and –OH) group leading to extend the conjugation [62–66]. A weak fluorescence intensity was observed at intermediate pH (HEPES buffer (20 mM, pH 7.4). Hence, the chemosensors DPSAD and IPSAD showed a significant response at a biologically relevant pH (7.4) which is very close to the physiological pH condition.

DFT Studies

DFT studies were performed for investigating to throw light on receptor-guest interaction mechanism. The optimized nature of the receptors (DPSAD and IPSAD) and the Zn^{2+}complex formed by co-ordination with receptors was obtained by DFT/B3LYP-6-31G and B3LYP/LanL2DZ basis set [67] respectively (Fig. 11). The fluorescence enhancement of receptor was easily understand after binding with Zn^{2+}, and also TD-DFT calculations were performed using DFT/B3LYP-6-31G basis set.

We carried out the quantum mechanical calculations in larger basis set. The representation is shown in Figs. 12 and Fig. 13 and the explanation is as follows, IPSAD is

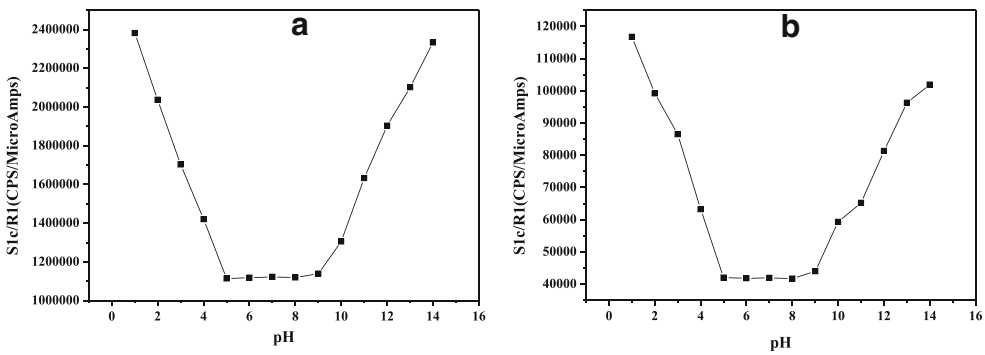

Fig. 10 Plot of fluorescence intensity against pH for DPSAD (**a**) and IPSAD (**b**) in THF/H_2O system

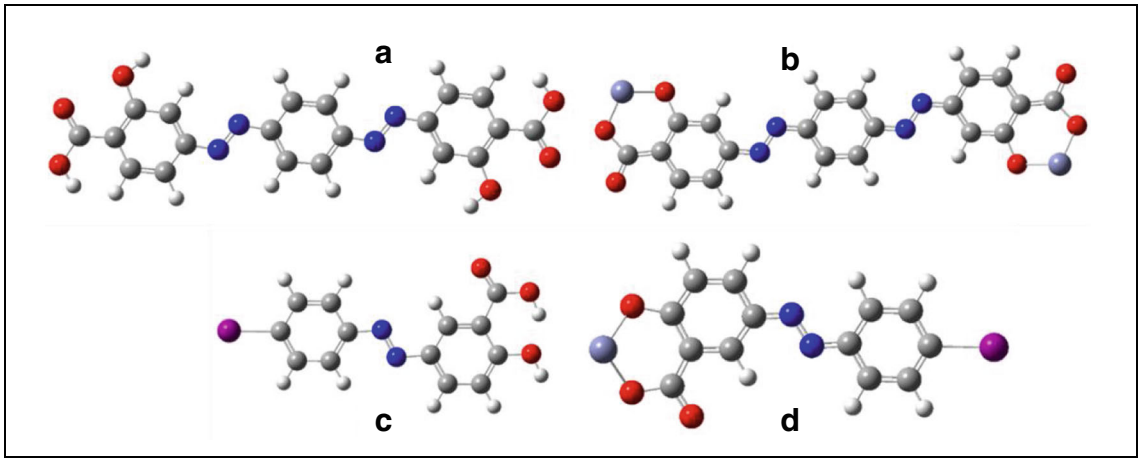

Fig. 11 Optimized structure of (**a**) DPSAD (**b**) DPSAD-Zn^{2+} (**c**) IPSAD (**d**) IPSAD- Zn^{2+}

an unsymmetrical compound. In the ground state, the electron distribution of IPSAD represents in the donor group of azo only. But in the excited state, the electron flows into the withdrawing group of carboxylic acid (acceptor). This transition clearly shows the charge transfer behaviour of IPSAD. After the addition of Zn^{2+} to IPSAD, the electron distribution is throughout the molecule in the ground state. In the excited state, electrons transferred into the metal to ligand through a chelation effect. The electrons are located in the ground state of

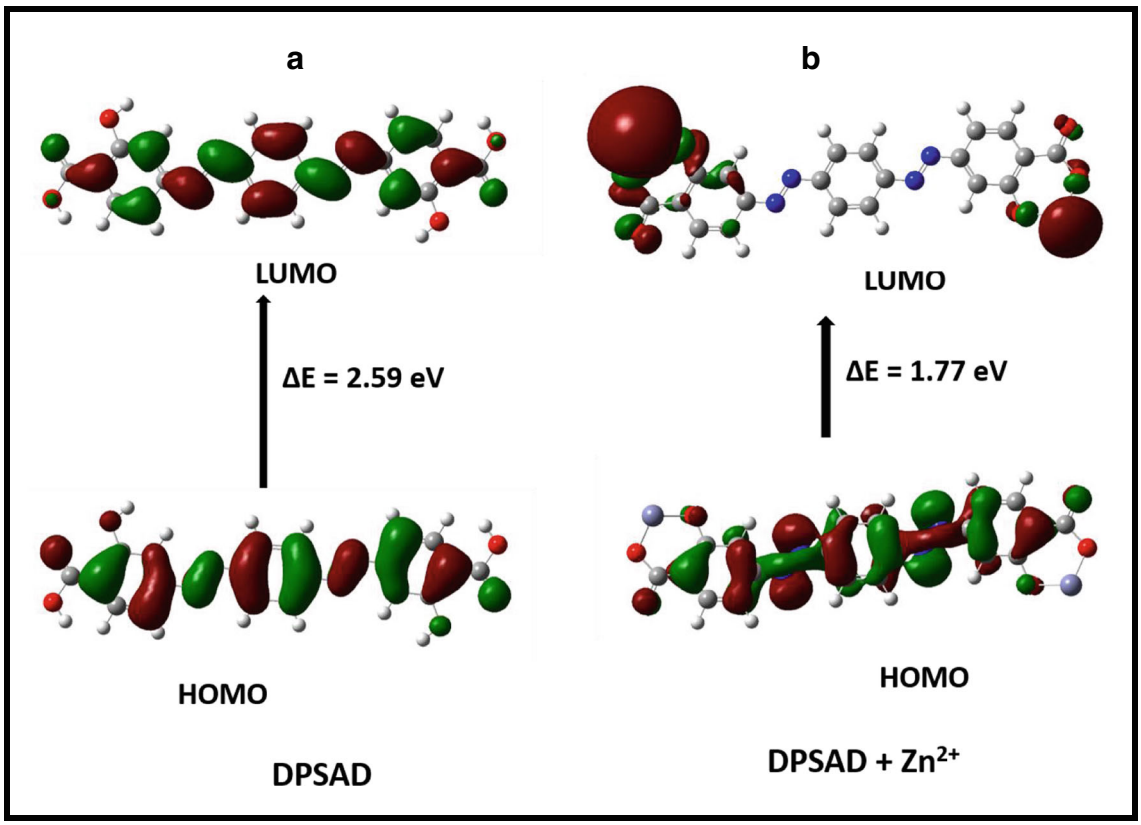

Fig. 12 DFT-computed molecular frontiers orbitals of DPSAD and DPSAD-Zn^{2+}

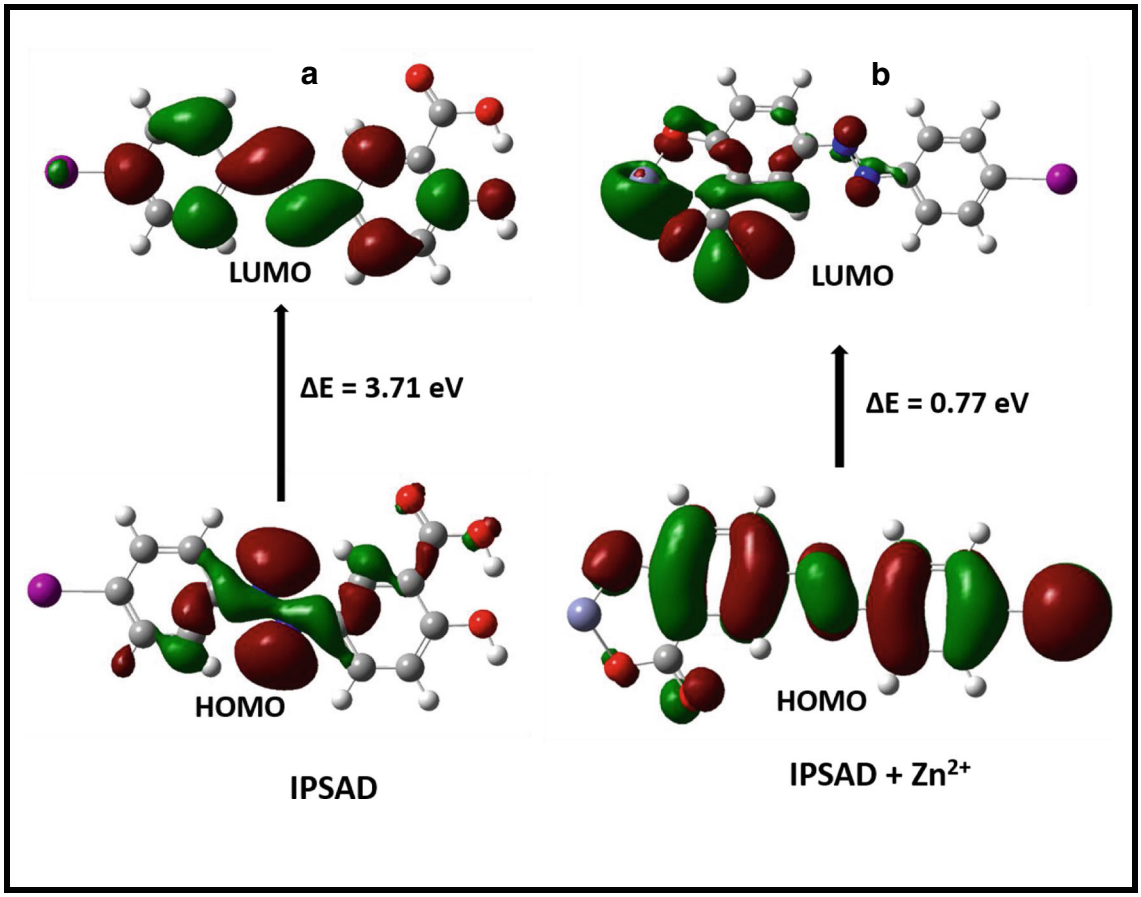

Fig. 13 DFT-computed molecular frontiers orbitals of IPSAD and IPSAD-Zn^{2+}

the symmetrical compound DPSAD on the azo side. When the molecules are excited, the electrons are transfered throughout the molecule due to charge transfer. Upon the addition of Zn^{2+} with DPSAD, the electrons are located throughout the molecule in the ground state but in the excited state electrons are

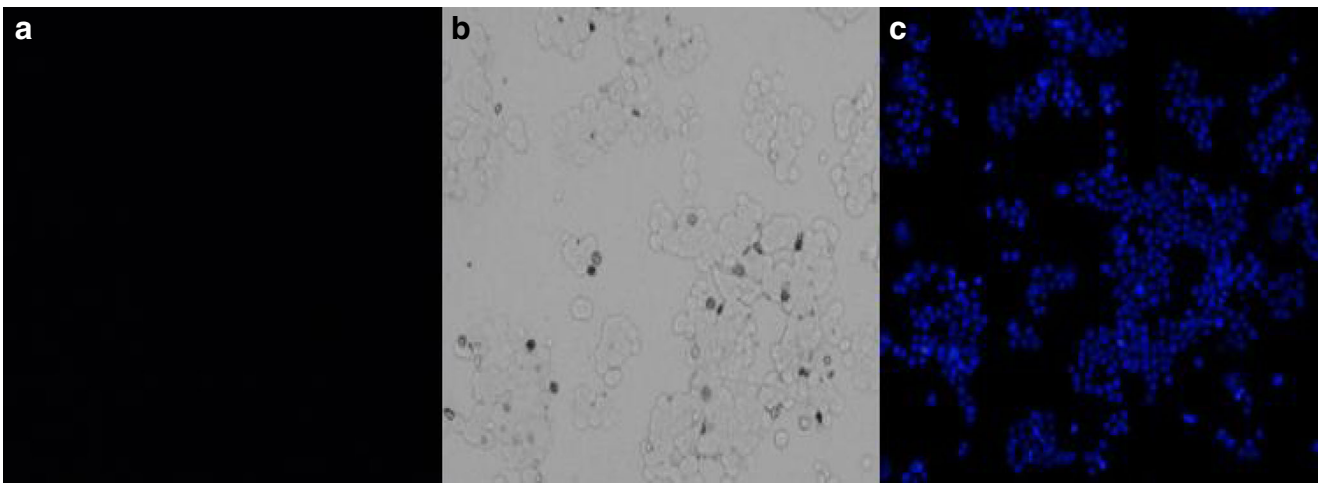

Fig. 14 Live-cell imaging of Zn^{2+} in HeLa cells; (**a**) fluorescence image of cells incubation with DPSAD (1 μM) for 30 min at 37 °C; (**b**) bright-field image of DPSAD treated HeLa cells; (**c**) fluorescence image of HeLa cells incubated with DPSAD (1 μM) and subsequently treated with $ZnCl_2$ (10 μM) for 15 min $\lambda_{emi} = 448$ nm

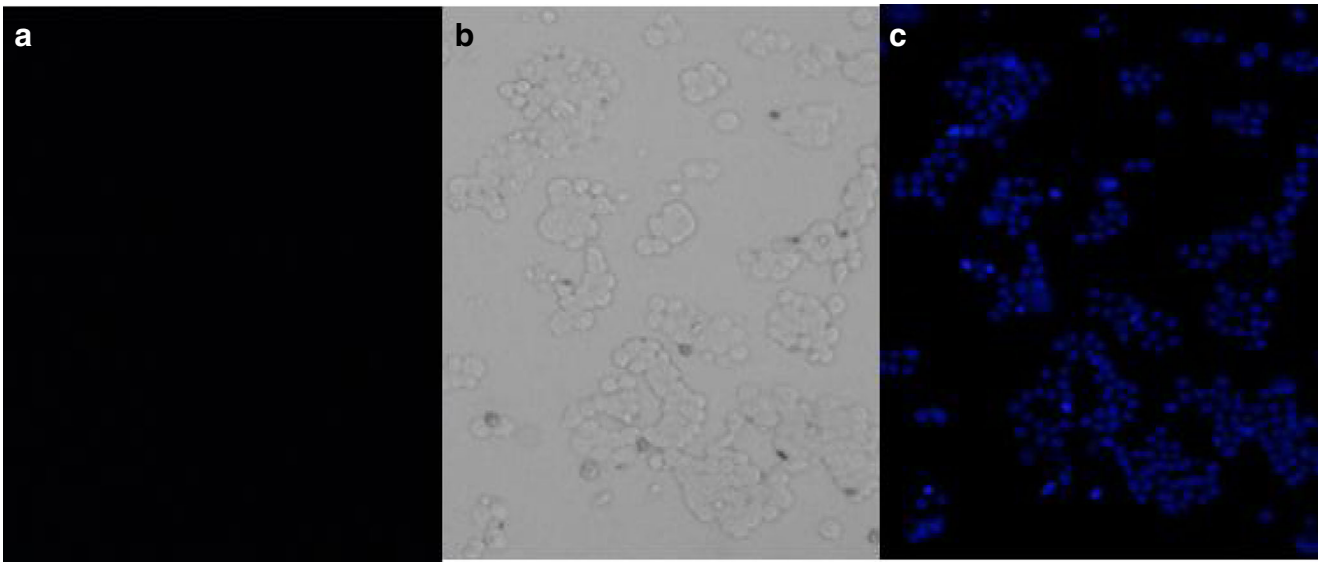

Fig. 15 Live-cell imaging of Zn^{2+} in Hela cells; (**a**) fluorescence image of cells incubation with IPSAD (1 μM) for 30 min at 37 °C; (**b**) bright-field image of IPSAD treated Hela cells; (**c**) fluorescence image of Hela cells incubated with IPSAD (1 μM) and subsequently treated with $ZnCl_2$ (10 μM) for 15 min $\lambda_{emi} = 406$ nm

transfered into the metal as well as acceptor of DPSAD molecule. This observation strongly supports the proposed mechanism.

Live Cell Imaging Studies

Due to the sensitivity of DPSAD and IPSAD, they preferably suitable for intracellular Zn^{2+} ion imaging in living cells. We have deliberated the sensitivity of DPSAD and IPSAD for Zn^{2+} in living HeLa cells by fluorescence microscopy. In primary stage, HeLa cells incubated with the receptors (DPSAD and IPSAD) did not show any fluorescence image (Figs. 14 and Fig. 15). After incubation of the receptor treated cells with Zn^{2+} ions, which shows the blue fluorescence observed and identified by the fluorescence microscope. From the observed results of fluorescence image shown that the fluorescence signals are localized on the intracellular region, which representing a good cell membrane permeability of chemosensors DPSAD and IPSAD. The blue fluorescence from the intracellular region proves that the receptors (DPSAD and IPSAD) are convincing for imaging Zn^{2+} in living cells. All these result shows that DPSAD and IPSAD are biocompatible in nature and it could be applied for detecting Zn^{2+} ions in cells quickly.

Conclusions

In summary, fluorescent chemosensors based on salicylate-azo derivatives have been designed and synthesized. The receptors reveal fluorescence turn-on response to Zn^{2+} in aqueous medium over the other competing metal ions. Density functional theory calculation shows that the observed fluorescence enhancement of receptors in the addition of Zn^{2+} is due to internal charge transfer mechanism. Furthermore, these molecules can be utilized in living cells for monitoring Zn^{2+} ions very effectively and quickly.

Acknowledgments The authors acknowledged to the Department of Science and Technology, SERB, Extramural Major Research Project (Grant No. EMR/2015/000969), Council of Scientific and Industrial Research (CSIR), HRDG, No. 01(2901)/17/EMR-II, New Delhi, Department of Science and Technology DST/TM/CERI/C130(G), New Delhi, India for financial support, and also we thank to DST-FIST, DST-PURSE and UPE for providing instrumental facilities.

References

1. Czarnik AW (1993) Fluorescent chemosensors for ion and molecular recognition. American Chemical Society, Washington DC
2. De Silva AP, Gunaratne HQN, Gunnlaugsson T, Huxley TM, McCoy CP, Rademacher JT, Rice TE (1997) Signaling recognition events with fluorescent sensors and switches. Chem Rev 97:1515–1566
3. Martinez-Manez R, Sancanon F (2003) Fluorogenic and chromogenic chemosensors and reagents for anions. Chem Rev 103:4419–4476
4. Gunnlaugsson T, Glynn M, Tocci GM, Kruger PE, Pfeffer FM (2006) Anion recognition and sensing in organic and aqueous media using luminescent and colorimetric sensors. Coord Chem Rev 250:3094–3117
5. Burdette SC, Walkup GK, Spingler B, Tsien RY, Lippard SJ (2001) Fluorescent sensors for Zn^{2+} based on a fluorescein platform: syn-

thesis, properties and intracellular distribution. J Am Chem Soc 123:7831–7841
6. Jiang P, Chen L, Lin J, Liu Q, Ding J, Gao X, Guo Z (2002) Novel zinc fluorescent probe bearing dansyl and aminoquinoline groups. Chem Commun:1424–1425
7. Ko S-K, Yang Y-K, Tae J, Shin I (2006) In vivo monitoring of mercury ions using a rhodamine-based molecular probe. J Am Chem Soc 128:14150–14155
8. Taki M, Desaki M, Ojida A, Lyoshi S, Hirayma T, Hamachi I, Yamamoto Y (2008) Fluorescence imaging of intracellular cadmium using a dual-excitation ratiometric chemosensor. J Am Chem Soc 130:12564–12565
9. Zhang X, Xiao Y, Qian X (2008) A ratiometric fluorescent probe based on FRET for imaging Hg^{2+} ions in living cells. Angew Chem Int Ed 47:8025–8029
10. Jiang P, Guo Z (2004) Fluorescent detection of zinc in biological systems: recent development on the design of chemosensors and biosensors. Coord Chem Rev 248:205–229
11. Wysockia LM, Lavis LD (2011) Advances in the chemistry of small molecule fluorescent probes. Curr Opin Chem Biol 15:752–759
12. Choi JY, Kim D, Yoon J (2013) A highly selective "turn-on" fluorescent chemosensor based on hydroxy pyrene-hydrazone derivative for Zn^{2+}. Dyes Pigments 96:176–179
13. Lippard SJ, Berg JM (1994) Principle of bioinogranic chemistry. University Science Book, CA
14. Andrews GK (2001) Cellular zinc sensors: MTF-1 regulation of gene expression. BioMetals 14:223–237
15. Burdette SC, Lippard SJ (2003) Meeting of the minds: metalloneurochemistry. Proc Natl Acad Sci U S A 100:3605–3610
16. Walker CF, Black RE (2004) Zinc and the risk for infectious disease. Annu Rev Nutr 24:255–275
17. Bush AI, Pettingell WH, Multhaup G, Paradis M, Vonsattel JP, Gusella JF, Beyreuther K, Masters CL, Tanzi RE (1994) Rapid induction of alzheimer a beta amyloid formation by zinc. Science 265:1464–1467
18. Koh J-Y, Suh SW, Gwag BJ, He YY, Hsu CY, Choi DW (1996) The role of zinc in selective neuronal death after transient global cerebral ischemia. Science 272:1013–1016
19. Voegelin A, Poster S, Scheinost AC, Marcus MA, Kretzschmar R (2005) Changes in zinc speciation in field soil after contamination with zinc oxide. Environ Sci Technol 39:6616–6623
20. Rensing C, Maier RM (2003) Issues underlying use of biosensors to measure metal bioavailability. Ecotoxicol Environ Saf 56:140–147
21. Ponnuvel K, Kumar M, Padmini V (2016) A new quinoline-based chemosensor for Zn^{2+} ions and their application in living cell imaging. Sensors Actuators B 227:242–247
22. Ponnuvel K, Padmini V, Sribalan R (2016) A new tetrazole based turn-on fluorescence chemosensor for Zn^{2+} ions and its application in bioimaging. Sensors Actuators B 222:605–611
23. Dong Z, Le X, Zhou P, Dong C, Ma J (2014) An "off-on-off" fluorescent probe for the sequential detection of Zn^{2+} and hydrogen sulfide in aqueous solution. New J Chem 38:1802–1808
24. Bao Y, Liu B, Du F, Tian J, Wang H, Bai R (2012) A new strategy for highly selective fluorescent sensing of F^- and Zn^{2+} with dual output modes. J Mater Chem 22:5291–5294
25. Kumar V, Kumar A, Diwan U, Upadhyay KK (2013) A Zn^{2+}-responsive highly sensitive fluorescent probe and 1D coordination polymer based on a coumarin platform. Dalton Trans 42:13078–13083
26. Iniya M, Jeyanthi D, Krishnaveni K, Mahesh A, Chellappa D (2014) Triazole based ratiometric fluorescent probe for Zn^{2+} and its application in bioimaging. Spectrochim Acta A Mol Biomol Spectrosc 120:40–46
27. Kiyose K, Kojima H, Urano Y, Nagano T (2006) Development of a ratiometric fluorescent zinc ion probe in near-infrared region, based on Tricarbocyanine chromophore. J Am Chem Soc 128:6548–6549
28. Guo Z, Kim G-H, Shin I, Yoon J (2012) A cyanine-based fluorescent sensor for detecting endogenous zinc ions in live cells and organisms. Biomaterial 33:7818–7827
29. Sivaraman G, Anand T, Chellappa D (2012) Turn-on fluorescent chemosensor for Zn (II) via ring opening of rhodamine spirolactam and their live cell imaging. Analyst 137:5881–5884
30. Jiang L, Wang L, Guo M, Yin G, Wang R-Y (2011) Fluorescence turn-on of easily prepared fluorescein derivatives by zinc cation in water and living cells. Sensors Actuators B 156:825–831
31. Sun W-C, Gee KR, Klaubert DH, Haugland RP (1997) Synthesis of fluorinated fluoresceins. J Organomet Chem 62:6469–6475
32. Zastrow ML, Radford RJ, Chyan W, Anderson CT, Zhang DY, Loas A, Tzounopoulos T, Lippard SJ (2016) Reaction-based probes for imaging mobile zinc in live cells and tissues. ACS Sens 1:32–39
33. Ojida A, Mito-Oka Y, Inoue M, Hamachi I (2002) First artificial receptors and chemosensors toward phosphorylated peptide in aqueous solution. J Am Chem Soc 124:6256–6258
34. Ertas N, Akkaya EU, Ataman OY (2001) Simultaneous determination of cadmium and zinc using a fiber optic device and fluorescence spectrometry. Talanta 51:693–699
35. Xu Z, Qian X, Cui J, Zhang R (2006) Exploiting the deprotonation mechanism for the design of ratiometric and colorimetric Zn^{2+} fluorescent chemosensor with a large red-shift in emission. Tetrahedron 62:10117–10122
36. Gunnlaugsson T, Lee TC, Parkesh R (2003) A highly selective and sensitive fluorescent PET (photoinduced electron transfer) chemosensor for Zn (II). Org Biomol Chem 1:3265–3267
37. Parkesh R, Lee TC, Gunnlaugsson T (2007) Highly selective 4-amino-1,8-naphthalimide based fluorescent photoinduced electron transfer (PET) chemosensors for Zn (II) under physiological pH conditions. Org Biomol Chem 5:310–317
38. Turfan B, Akkaya EU (2002) Modulation of boradiazaindacene emission by cation-mediated oxidative PET. Org Lett 4:2857–2859
39. Harriman A, Mallon LJ, Stewart B, Ulrich G, Ziessel R (2007) Boron dipyrromethene dyes bearing ancillary 2,2′:6′,2″-terpyridine coordination sites. Eur J Org Chem 2007:3191–3198
40. Scheller FW, Schubert F, and Fedrowitz J. (1997) Frontiers in biosensors I: fundamental aspects. Bosal Boston Berlin Birkauser
41. Wang W, Gao S, Wang B (2002) Boronic acid-based sensors. Curr Org Chem 6:1285–1317
42. Jiang W, Fu Q, Fan H, Wang W (2008) An NBD fluorophore-based sensitive and selective fluorescent probe for zinc ion. Chem Commun:259–261
43. Xu Z, Kim G-H, Han SJ, Jou MJ, Lee C, Shin I, Yoon J (2009) An NBD-based colorimetric and fluorescent chemosensor for Zn^{2+} and its use for detection of intracellular zinc ions. Tetrahedron 65:2307–2312
44. Helal A, Lee SH, Kim SH, Kim H-S (2010) Dual-signaling fluorescent chemosensor based on bisthiazole derivatives. Tetrahedron Lett 51:3531–3535
45. Atilgan S, Ozdemir T, Akkaya EU (2008) A sensitive and selective ratiometric near IR fluorescent probe for zinc ions based on the distyryl-bodipy fluorophore. Org Lett 10:4065–4067
46. Xu Z, Yoon J, Spring DR (2010) Fluorescent chemosensors for Zn^{2+}. Chem Soc Rev 39:1996–2006
47. Wang L, Quin W, Tang X, Dou W, Liu W (2011) Development and applications of luorescent indicators for Mg^{2+} and Zn^{2+}. J Phys Chem A 115:1609–16016
48. Huang X, Miao Q, Wang L, Jiao J, He X, Cheng Y (2013) A highly sensitive and selective fluorescence chemosensor for Cu^{2+} and Zn^{2+} based on solvent effect. Chin J Chem 31:195–199
49. Ashokkumar P, Ramakrishnan VT, Ramamurthy P (2011) Photoinduced electron transfer (PET) based Zn^{2+} fluorescent probe: transformation of turn-on sensors into ratiometric ones with dual emission in acetonitrile. J Phys Chem A 115:14292–14299
50. Bae SW, Kim E, Shin I-S, Park SB, Hong J-I (2013) Fluorescent chemosensor for biological zinc ions. Supramol Chem 25:2–6

51. Lu X, Zhu W, Xie Y, Li X, Gao Y, Li F, Tian H (2010) Near-IR core-substituted naphthalenediimide fluorescent chemosensors for zinc ions: ligand effects on PET and ICT channels. Chem Eur J 16:8355–8364
52. Li M, Lu H-Y, Liu R-L, Chen J-D, Chen C-F (2012) Turn-on fluorescent sensor for selective detection of Zn^{2+}, Cd^{2+}, and Hg^{2+} in water. J Organomet Chem 77:3670–3673
53. Zhang Q-Q, Yang B-X, Sun R, Ge J-F, Xu Y-J, Li N-J, Lu J-M (2012) A near-infrared phenoxazinium-based fluorescent probe for zinc ions and its imaging in living cells. Sensors Actuators B 171-172:1001–1006
54. Cotton FA, Wilkinson G (1988) Advances in inorganic chemistry, 5th edn. Wiley, New York, p 957
55. Zhu S, Zhang J, Janjanam J, Vegesna G, Luo F-T, Tiwari A, Liu H (2013) Highly water-soluble BODIPY-based fluorescent probes for sensitive fluorescent sensing of zinc (II). J Mater Chem B 1:1722–1728
56. Wen X, Wang Q, Fan Z (2018) Highly selective turn-on fluorogenic chemosensor for Zn (II) detection based on aggregation-induced emission. J Lumin 194:366–373
57. Shi Z, Tu Y, Pu S (2018) An efficient and sensitive chemosensor based on salicylhydrazide for naked-eye and fluorescent detection of Zn^{2+}. RSC Adv 8:6727–6732
58. Kaleeswaran D, Murugavel R (2018) Picric acid sensing and CO2 capture by a sterically encumbered azo-linked fluorescent triphenylbenzene based covalent organic polymer. J Chem Sci (Berlin, Ger) 130:41640
59. Balasaravanan R, Sadhasivam V, Sivaraman G, Siva A (2016) Triphenylamino α-cyanovinyl-and cyanoaryl-based fluorophores: solvatochromism, aggregation-induced emission and electrochemical properties. Asian J Org Chem 5:399–410
60. Sivamani J, Balasaravanan R, Duraimurugan K, Siva A (2016) Synthesis, characterization and photophysical studies of self-assembled azo biphenyl urea derivatives. Photochem Photobiol Sci 15:211–218
61. Shortreed M, Kopelman R, Kuhn M, Hoyland B (1996) Fluorescent fiber-optic calcium sensor for physiological measurements. Anal Chem 68:1414–1418
62. Lee JJ, Lee SA, Kim H, Nguyen LT, Noh I, Kim C (2015) A highly selective CHEF-type chemosensor for monitoring Zn^{2+} in aqueous solution and living cells. RSC Adv 5:41905–41913
63. Goswami S, Das AK, Aich K, Manna A, Maity S, Khanra K, Bhattacharyya N (2013) Ratiometric and absolute water-soluble fluorescent tripodal zinc sensor and its application in killing human lung cancer cells. Analyst 138:4593–4598
64. Lv Y, Cao M, Li J, Wang J (2013) A sensitive ratiometric fluorescent sensor for zinc (II) with high selectivity. Sensors 13:3131–3141
65. Iniya M, Jeyanthi D, Krishnaveni K, Chellappa D (2015) A bifunctional chromogenic and fluorogenic probe for F^- and Al^{3+} based on azo-benzimidazole conjugate. J Lumin 157:383–389
66. Anand T, Sivaraman G, Mahesh A, Chellappa D (2015) Aminoquinoline based highly sensitive fluorescent sensor for lead (II) and aluminium (III) and its application in live cell imaging. Anal Chim Acta 853:596–601
67. Fox DJ (2009) Gaussian 09 revision a.02. Gaussian Inc, Wallingford